

# Numerical modelling of fixed-bed co-gasification process through Multiple Thermally Thick Particle (MTTP) model

Linzhen Wang  
School of Mechanical Engineering  
Shanghai Jiao Tong University  
Shanghai, China  
wlz1997@sjtu.edu.cn

Ruiqu Deng  
School of Mechanical Engineering  
Shanghai Jiao Tong University  
Shanghai, China  
fjlydrq@sjtu.edu.cn

Ruizhi Zhang  
School of Mechanical Engineering  
Shanghai Jiao Tong University  
Shanghai, China  
zhang.ruizhi@sjtu.edu.cn

Yonghao Luo\*  
School of Mechanical Engineering  
Shanghai Jiao Tong University  
Shanghai, China  
yhluo@sjtu.edu.cn

*Abstract*—Co-gasification technology provides a feasible solution for the energetic valorization of various types of biomass feedstocks, especially those not directly applicable for gasification owing to their low-calorific values or high ash content. Numerical modelling is a promising approach to evaluate the performance and analyze the conversion processes inside the gasifier, but the complexity of co-gasification technology has put forward challenges to the model formulation. This paper established the Multiple Thermally Thick Particle (MTTP) model for simulating the co-gasification process. MTTP model could not only calculate the individual conversion processes of different fuels, but also simultaneously reflect the characteristics of thermally thick particles and the interactions between different fuels through sub-grid models for the solid phase. Experimental results of a downdraft fixed-bed co-gasification from literature were adopted for model validation. The modelling results from the MTTP model are in good agreement with the measured values of temperature and syngas composition upon changing the co-gasification ratio (CGR). Further analysis of the weight-loss process of different fuel particles and the corresponding intraparticle temperature distribution have confirmed the different conversion characteristics and interactions between different fuels during co-gasification process.

*Keywords*—Co-gasification, Downdraft fixed-bed gasifier, Numerical modelling, Thermally-thick particle, Sub-grid model

## I. INTRODUCTION

Currently there is an increasing trend in using biomass as a carbon neutral energy source to reduce our dependence on fossil fuels. Thermo-chemical conversion is a promising route to realize efficient and sustainable utilization of biomass, and fixed-bed gasification is a key technology of thermochemical conversion processes to convert solid biomass into combustible gases, which is especially suitable for decentralized utilization of biomass. Energetic valorization of

various types of biomass feedstocks is also capable of mitigating the environmental impact of massive waste production, such as agricultural and forestry residues [1], plastics wastes [2] and poultry Litter [3].

Considering that the wide varieties of biomass materials have different physical characteristics and chemical compositions, some feedstocks are not directly applicable for gasification owing to their low-calorific values or high ash content. Co-gasification provides a feasible solution for utilizing these low-quality feedstocks, improving the flexibility and efficiency of gasification technology [4]. For instance, co-gasification of bituminous coal and industrial sludge could solve the problem of unstable calorific value of industrial sludge [5], and co-gasification of high ash-containing feedstocks (like MSW) and biomass has the potential of reducing the overall ash content and the fusion of ash, mitigating the ash agglomeration in the reactor bed [6]. However, the quality of final products of gasification largely depends on process types and operating parameters, including temperatures, particle size and waste type.

In recent years, researchers have intensified their work to improve the performance of the gasifier using numerical modelling [7]. Among the various approaches for modeling the gasification process, computational fluid dynamics (CFD) is a sophisticated and robust tool, which could not only evaluate the overall performance and efficiency but also analyze the complex conversion processes inside the gasifier [8]. However, the reliable numerical results require reasonable simplification and description of the physiochemical processes inside the gasifier, and the co-gasification of different biomass feedstocks has put forward challenges for model formulation.

In practice, different feedstocks may have different size distribution, ranging from millimeter-sized to centimeter-sized [9,10]. Particle size directly determines the thermal history of fuel particles, consequently influencing the onset and duration of different conversion processes. In particular, centimeter-sized fuel particles are commonly used, but most numerical works treat them as thermally thin particle, which

could not precisely reflect the influence of heat transfer resistance and intraparticle conversion processes [11, 12]. Meanwhile, different feedstocks may have different fuel composition and properties, such as moisture content, pyrolysis kinetics and char reactivity. The profiles temperature and gas composition could be altered when changing the mixing rate, and the regions of different conversion stages could overlap with each other. Some numerical models adopted averaged fuel properties to treat the mixed feedstock [13], which may result in significant deviation between modelling results and measured values.

In this work, we present the Multiple Thermally Thick Particle (MTTP) model for analyzing the fixed-bed co-gasification process. This model extended the conventional Eulerian-Eulerian type multiphase model, further dividing the solid phase into several sub-phases, representing the different layers of fuel particle. The governing equations of mass and energy conservation are formulated for each solid sub-phases, and the source terms are calculated strictly based on the intraparticle transport and conversion processes. The model framework of MTTP is easily extensible, not only for multiple kinds of fuels, but also suitable for modelling the co-combustion and co-pyrolysis process. The accuracy of the MTTP is validated based on the co-gasification experiments performed by Bhoi et al. [9] in a commercial scale downdraft gasifier.

## II. MODEL ESTABLISHMENT

### A. Fuel properties

In the experimental works by Bhoi et al. [9], two different feedstocks were utilized, including MSW pellets of 16 mm diameter and 25 mm length, and switchgrass crushed by a tub grinder. For simplification of modelling, the fuel particles are regarded as spheres, and the initial diameter of MSW pellet and switchgrass are assumed to be 20 mm and 5 mm, respectively. The fuel properties are listed in Table I.

TABLE I. PROPERTIES OF MSW PELLET AND SWITCHGRASS.

Proximate (Wt.%)	MSW pellet	Switchgrass
Moisture content (wb)	3.80	7.70
Volatile matter (db)	77.54	78.60
Fixed carbon (db)	8.72	17.47
Ash (Wt. %, db)	13.74	3.93
Ultimate (Wt. %, db)		
Carbon, C	50.71	49.63
Hydrogen, H	6.13	5.72
Oxygen, O	29.14	40.37
Nitrogen, N	0.14	0.30
Sulphur, S	0.14	0.05

Three working conditions were tested with different co-gasification ratios (CGR, 0%, 20% and 40%), which is defined as the mass fractions of MSW pellet in the fuel mixture. The excess air ratio is controlled at 0.22, and the bio-char extraction rate of the ash scrapper is controlled at 40.0 kg/h for all the cases. Detailed settings of working conditions and the schematic of the downdraft gasifier system could refer to their original paper [9].

### B. Model framework

The co-gasification process is simulated with a 1-D model for the gasifier coupled with sub-grid particle models, as is shown in Fig. 1. In the MTTP, the fuel bed is treated as a disperse porous medium, which contains a gas phase and several solid sub-phases. The particles are identical for the same fuel in each computational cell, but the composition and conversion status of different fuels are separately calculated in a shrinking-core regime.

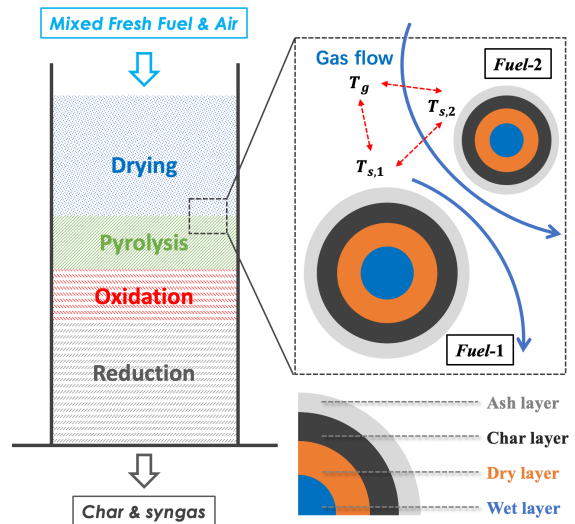


Fig. 1. Schematic diagram of the co-gasification processes and particle structure

The fuel particles were divided into four connected layers, including wet layer, dry layer, char layer and ash layer, and the internal layers are modeled as concentric spheres. In each layer, the material properties are constant. The wet layer of each fuel is composed of moisture, volatile, char and ash following the relative content from proximate analysis. Similarly, the dry layer contains volatile, char and ash, and the char layer is composed of char and ash. The outer layer is purely ash. Initially the fuel particle is almost all wet layer, and 0.1% of initial mass are assigned to other layers at the beginning.

Inside the fuel bed, the heat transfer processes include gas-solid convective heat transfer, gas-solid radiative heat transfer, and solid-solid radiative heat transfer. The conductive heat transfer is only considered inside the fuel particle between different layers, and therefore the direct-contact heat transfer between solid phase is neglected. Inside a computational grid, the environmental heat source from convective and radiative heat transfer is allocated to different fuels according to the ratio of surface area.

During conversion process, drying is assumed to occur at the boundary of wet layer, and the pyrolysis process occurs inside the dry layer. Char heterogeneous reactions occur at the boundary of the char layer, which causes the accumulation of ash layer. Inside the fuel particle the heat is transferred by conduction, and for the ash layer, the convective and radiative heat transfer with the gas phase and the surrounding solid particles are also considered. With two different fuels taken into consideration, there are eight solid sub-phases in the porous medium, and for each phase the governing equations of mass and energy conservation are established.

### C. Governing equations

In conventional Eulerian-Eulerian model, the solid phase is treated as pseudo-fluid so that the governing equations of mass and energy conservation share the same general form as the gas phase [14]. The MTTP model is an extended Eulerian-Eulerian multiphase model, and therefore for each solid sub-phases the mass and energy conservation could also be established as pseudo-fluids, as is shown in Fig. 2. The total porosity is assumed to be constant, but the volume fraction of each solid sub-phase may continuously change during the conversion process. For instance, when drying occurs, the fraction of wet sub-phase would decline, and the corresponding drying sub-phase would increase. Therefore, the local particle structure could be reflected by the fractions of each sub-phases.

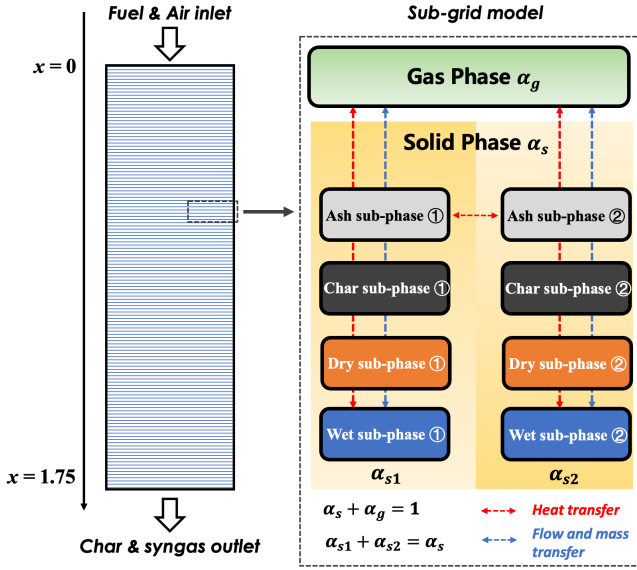


Fig. 2. Schematic diagram of the sub-grid models.

For the gas phase in the porous medium, the governing transport equations include continuity, momentum, energy, and species conservations. The turbulence is treated by k-ε model.

$$\frac{\partial}{\partial t}(\varepsilon \rho_g) + \frac{\partial}{\partial x_j}(\varepsilon \rho_g u_{j,g}) = S_s \quad (1)$$

$$\frac{\partial}{\partial t}(\varepsilon \rho_g u_{i,g}) + \frac{\partial}{\partial x_j} \left[ \varepsilon \rho_g u_{i,g} u_{j,g} - \mu \left( \frac{\partial u_{i,g}}{\partial x_j} \right) \right] = S_{i,M} + S_i(U_{i,g}) \quad (2)$$

$$\frac{\partial}{\partial t}(\varepsilon \rho_g \bar{c}_{p,g} T_g) + \frac{\partial}{\partial x_j}(\varepsilon \rho_g \bar{c}_{p,g} u_{j,g} T_g) = \frac{\partial}{\partial x_j} \left( \lambda_{eff,g} \frac{\partial T_g}{\partial x_j} \right) + S_{Q,g} \quad (3)$$

$$\frac{\partial}{\partial t}(\varepsilon \rho_g Y_{i,g}) + \frac{\partial}{\partial x_j}(\varepsilon \rho_g u_{j,g} Y_{i,g}) = \frac{\partial}{\partial x_j} \left( \rho_g D_{g,eff} \frac{\partial Y_{i,g}}{\partial x_j} \right) + M_{i,g} + M_{i,s} \quad (4)$$

The solid phase is composed of two different fuels, and each fuel particle has four layers. Therefore, there are in total eight sub-phases in the solid phase. For the  $k^{\text{th}}$  layer of  $N^{\text{th}}$  fuel, the general form of mass conservation could be expressed as:

$$\frac{\partial}{\partial t}[(1-\varepsilon)\alpha_{s,k,N}\rho_{s,k,N}] + \frac{\partial}{\partial x_j}[(1-\varepsilon)\alpha_{s,k,N}\rho_{s,k,N}u_{j,s}] = S_{s,k,N}, \quad (5)$$

in which  $\alpha_{k,N}$  refers to the volumetric ratio of each sub-phase in the whole solid phase, and the source term  $S_{s,k,N}$  depends on the reaction process of the present layer and the neighboring layer.

The general form of energy balance for the  $k^{\text{th}}$  layer of  $N^{\text{th}}$  fuel could be expressed as:

$$\frac{\partial}{\partial t}[(1-\varepsilon)\alpha_{s,k,N}\rho_{s,k,N}\bar{c}_{p,s}T_{s,k,N}] + \frac{\partial}{\partial x_j}[(1-\varepsilon)\alpha_{s,k,N}\rho_{s,k,N}\bar{c}_{p,s}u_{j,s}T_{s,k,N}] = S_{Q,k,N}, \quad (6)$$

in which the source term  $S_{Q,k,N}$  is formed by the addition of five different heat sources:

$$S_{Q,k,N} = S_{reac,k,N} + S_{Cond,k,N} + S_{Env,k,N} + S_{Blowing,k,N} + S_{Evolution,k,N} \quad (7)$$

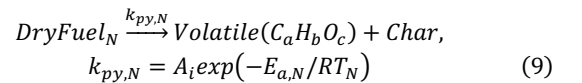
For the  $k^{\text{th}}$  layer of  $N^{\text{th}}$  fuel,  $S_{reac,k,N}$  represents the heat generation and consumption due to the solid reactions,  $S_{Cond,k,N}$  represents the heat conduction with neighboring layers calculated based on Fourier's rule,  $S_{Env,k,N}$  represents the heat exchanged between the particle and the environment through convection and radiation,  $S_{Blowing,k,N}$  is caused by the expulsion of the gases from the inner layers, and finally  $S_{Evolution,k,N}$  stands for the enthalpy exchange with the interior and exterior layers owing to conversion of solid phase materials. In the present model, the shrinkage of solid phase particle is neglected, and therefore the velocity of the solid phase depends on the char extraction rate at the ash outlet.

### D. Reaction models

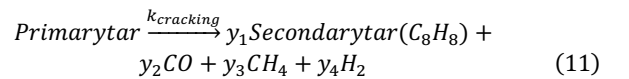
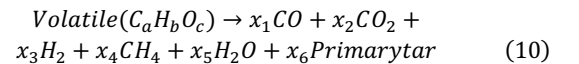
In the solid phase, the conversion processes include the drying, pyrolysis and char reactions. For the drying process, both the equilibrium model and thermal model were considered.

$$r_{drying} = \begin{cases} A_s h_s (C_{w,s} - C_{w,g}) & \text{if } T < 373K \\ Q_{cr}/H_{evap} & \text{if } T \geq 373K \end{cases} \quad (8)$$

The pyrolysis process of each fuel is modeled with one-step global reaction:



The volatile ( $C_a H_b O_c$ ) is released to the gas phase immediately after pyrolysis, and a volatile break-up approach is adopted to calculate the specific composition of the volatiles:



Detailed algorithm of calculating the volatile composition has been presented by Ngamsidhipongsa et al. [15].

For the overall reaction rate of heterogeneous char reactions, the kinetics reaction rate  $R_{k,m}$ , gas film diffusion  $R_{g,m}$  and ash-film diffusion  $R_{Ash}$  were all considered at the gas-solid interface:

$$r_{char,m} = \left( \frac{MW_i}{v_i} \right) \frac{\rho_{char}}{1/R_{k,m} + 1/R_{g,m} + 1/R_{Ash}}, \quad (12)$$

in which  $m$  denotes the types of gasification agent ( $O_2$ ,  $CO_2$  and  $H_2O$ ).

In the gas phase, the gaseous species includes  $CO_2$ ,  $CO$ ,  $H_2O$ ,  $H_2$ ,  $CH_4$ ,  $O_2$ , and details of the kinetic rates of homogeneous reactions could refer to Yao et al. [16]. The overall reaction rates are equal to the minimum value of turbulent mixing rates and kinetics reaction rates:

$$r_{vol,k} = \min(r_{g,k}, r_{tm,k}), \quad (13)$$

in which the turbulent mixing rate is expressed based on Eddy Dissipation Model (EDM).

### III. RESULTS AND DISCUSSIONS

#### A. Model validation with experimental measurements

The temperature distributions of gas phase along the axis direction under different mixing ratios are shown in Fig. 3. In the experiments, it is reported that the average gasification temperatures varied in the range of about 700-900 °C with an average temperature of approximately 800 °C, and gasification temperatures marginally reduced as the CGR increased from 0 to 40%. The predicted temperature lies in the same range of experiments, and the modelling results have also well reflected the declining trend of temperature when increasing the GCR. It is obvious that the onset of fast temperature increase at the oxidation zone was postponed as more fuel particles with large particle size was mixed in the feedstock. For  $GCR=0\%$ , the small fuel particles may dry up very fast near the oxidation zone, and the pyrolysis process is then intensified, leading to the highest temperature near the oxidation zone. The smaller particle size is also advantageous for heterogeneous char gasification reactions owing to the larger surface area inside the fuel bed, and therefore the temperature decreases faster for  $GCR=0\%$  than other working conditions.

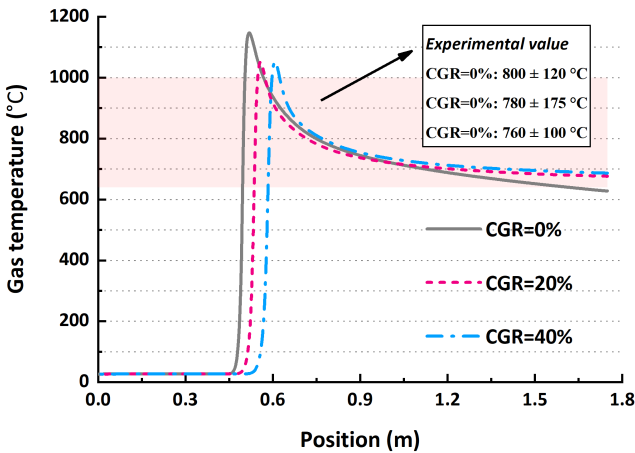


Fig. 3. Temperature distribution of gas phase along the axis direction under different mixing ratios.

The different temperature distributions indicate that changing the mixing ratio is likely to alter the conversion processes inside the gasifier. The downdraft gasifier is often divided into four neighboring zones, including drying, pyrolysis, oxidation and reduction zone. In practice, the design and working conditions are often determined based on the

location of these zones, which requires accurate prediction of temperature distribution, especially when the properties of inlet fuels are changed. The modelling results of MTTP are in good agreement with the experimental observations, which is beneficial for optimizing the design and choosing the proper working conditions.

The syngas compositions under different mixing ratios are shown in Fig. 4. Since the air and fresh fuels were moving in the same direction, the oxygen content quickly decreased with the onset of oxidation process, and the relative content of all the combustible gases gradually increased. The predicted content of  $CO_2$ ,  $CO$ ,  $H_2$  and  $CH_4$  were compared with the measured results at the outlet of gasifier. In general, the numerical results are close to the measured results. The relative errors are acceptable since the actual gas composition would fluctuate owing to the change of fuel properties and operation errors in experiments. When increasing the mixing ratio of MSW, the average content of  $CO_2$  and  $CO$  at the outlet gradually decreased, which is probably due to the decrement of O content in the feedstocks, as is shown in TABLE I. Correspondingly, the content of  $H_2$  gradually increased. In the experimental works by Bhoi et al. [9], the relative contents of other hydrocarbons are also measured, such as  $C_2H_2$ ,  $C_2H_4$  and  $C_2H_6$ . Owing to the simplification in calculating the composition of volatile, only  $CH_4$  is considered in the present model, for which the modelling results are also very close to the measured value.

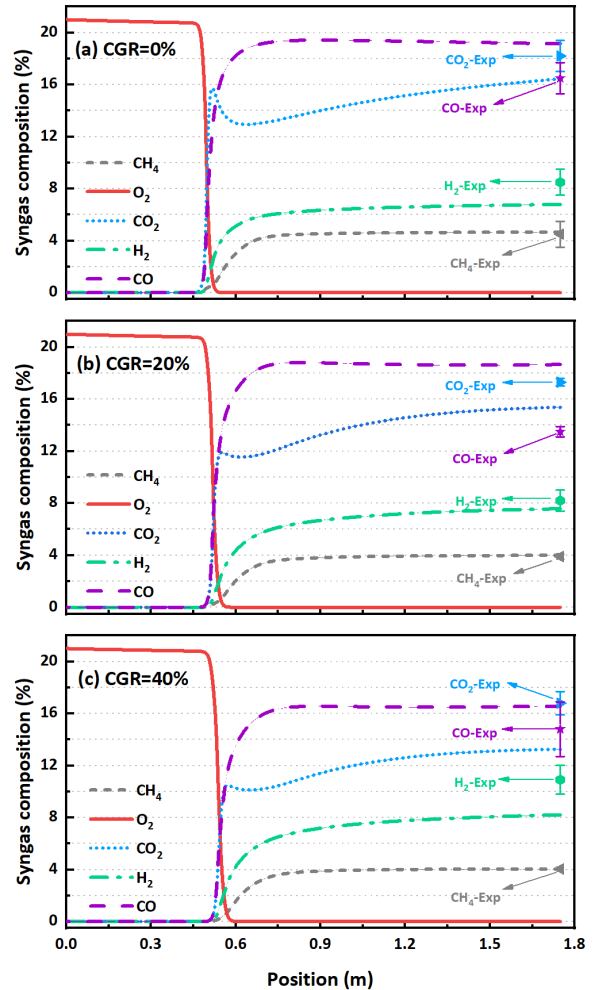


Fig. 4. Syngas compositions under different mixing ratios.

### B. Analysis of particle-scale conversion characteristics

When using fuel particles with different sizes and fuel properties, their conversion processes could differ from each other even at the same position. This phenomenon is crucial for co-gasification process since the position of the conversion zones inside the gasifier is often determined for a single fuel. When different fuels are mixed, they may exhibit different weight-loss history, and consequently the different conversion zones may overlap with each other. This effect may also be magnified when large fuel particles are utilized. Therefore, it would be meaning full to further analyze the conversion characteristics at particle scale. The conversion ratio of the fuel particle is defined as

$$\text{Conversion ratio} = \frac{M_{ini} - M_p}{M_{ini}}, \quad (14)$$

in which  $M_{ini}$  represents the initial particle mass, and  $M_p$  stands for the particle mass at a certain position. The weight-loss curves of different fuels is shown in Fig. 5.

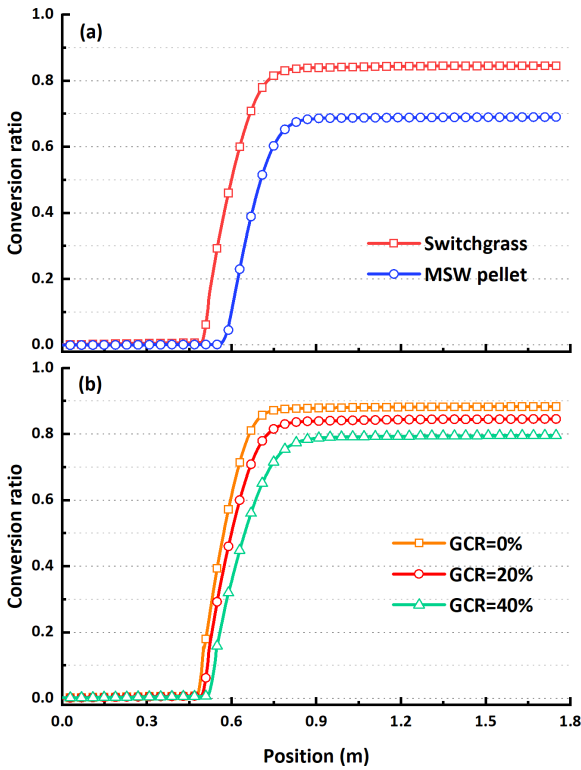


Fig. 5. Weight-loss curves of different fuels. (a) Switchgrass and MSW pellet at GCR = 20%; (b) Switchgrass at different GCRs.

Fig.5(a) shows the weight-loss curves of switchgrass and MSW pellet at GCR = 20%. Apparently, switchgrass with an initial particle size of 5 mm started to convert earlier than MSW pellet with an initial particle size of 25 mm, which could be attributed to the lower heat transfer resistance of solid phase and quicker drying process. The final conversion ratio of switchgrass is 0.83, which is only 0.69 for MSW pellet. The smaller particle size of switchgrass provides larger surface area inside the fuel bed, thus intensifying the char oxidation and gasification. Meanwhile, the ash content of MSW pellet (13.74 wt.%) is significantly higher than switchgrass (3.93 wt.%), which could also hinder the penetration of oxidants to char surface. This effect is included in the numerical model by adding the ash-film diffusion term in the expression of heterogeneous char reaction rate.

Fig.5(b) shows the weight-loss curves of switchgrass at different GCRs. The addition of MSW pellet could to some extent delay the conversion process of switchgrass, which indicated the interactions between different fuels. In general, the weight-loss become slower when more MSW pellet is added in the mixture, and the final conversion ratio is also decreased. The presence of another fuel could influence the conversion process of switchgrass at least in two ways. For one thing, owing to the different heat transfer resistance and duration of drying process, the surface temperatures of each fuel may be different even at the same location. Therefore, the low-temperature particle could lower the surface temperature of another one. For another, when the ER is fixed, different fuels would compete for the limited oxidants, which may also influence the individual conversion process of each fuel.

For thermally thick fuel particles, the most prominent characteristic is the intraparticle temperature gradient, which would cause the co-existence of different conversion stages in a single fuel particle [17]. Fig. 6 shows the intraparticle temperature distributions of different fuels. For switchgrass, the drying process terminated very soon and the difference in temperature between each layer is not significant. On the contrary, for MSW pellets, the drying process lasted from  $x$  position of 0.55 m to 0.66 m. During this process, the temperature of the wet layer was kept at the boiling temperature (100 °C), and consequently the temperatures of the dry layer and the char layer were relatively lowered until the end of drying process. The modelling results could clearly reveal the characteristics of thermally thick fuel particles, which explained why the onset of fast temperature increase at the oxidation zone was postponed as more MSW were added in the feedstock.

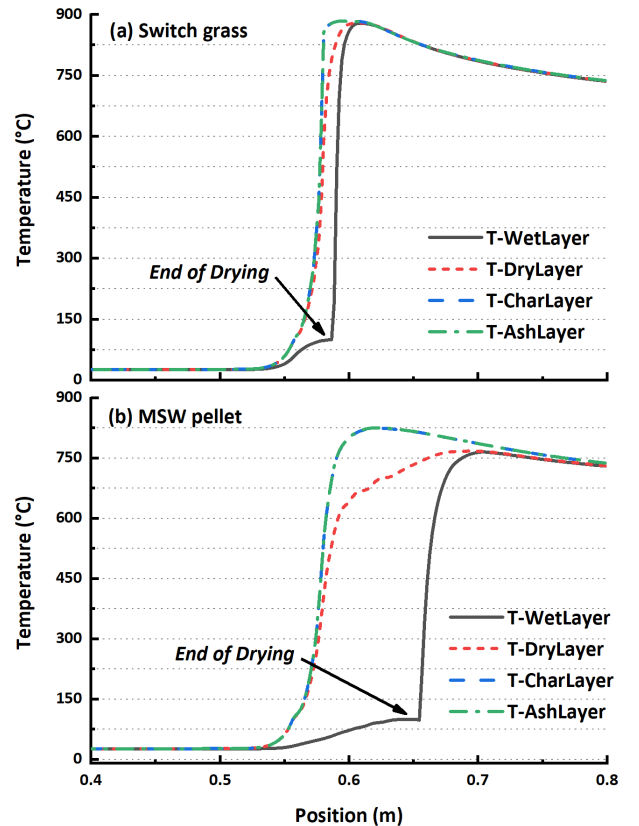


Fig. 6. Intraparticle temperature distributions of different fuels.

#### IV. CONCLUSION

In the present work, the co-gasification process of switchgrass and MSW pellet in a fixed-bed downdraft gasifier is simulated through the Multiple Thermally Thick Particle (MTTP) model. The modelling results of temperature and syngas composition are in good agreement with the measured values upon changing the co-gasification ratio (CGR), and the weight-loss processes of different fuels were also comparatively analyzed, together with the intraparticle temperature distribution. The main conclusions are as follows.

1) When the particle sizes are significantly different, changing the CGR would influence the overall gasification characteristics since fuel particles with large and small sizes would exhibit different weight-loss history.

2) Sub-grid model for thermally thick fuel particle could clearly reveal the temperature gradient inside the fuel particle, especially when the drying process is not terminated, which could directly influence the onset of conversion processes.

3) Co-gasification would cause interactions between different fuels, and modelling results have shown that higher ratio of MSW pellets with large particle size would delay the conversion process of switchgrass.

#### ACKNOWLEDGMENT

The authors would like to acknowledge the financial support from the National Natural Science Foundation of China [51706139] and the Science and Technology Commission of Shanghai Municipality [20dz1203304].

#### REFERENCES

- [1] Kang K, Klinghoffer N B, ElGhamrawy I, Berruti F. Thermochemical conversion of agroforestry biomass and solid waste using decentralized and mobile systems for renewable energy and products. *Renewable and Sustainable Energy Reviews*, 2021, 149: 111372-91.
- [2] Nanda S, Berruti F. Thermochemical conversion of plastic waste to fuels: a review. *Environmental Chemistry Letters*, 2021, 19(1): 123-148.
- [3] Bora R R, Lei M, Tester J W, Johannes Lehmann, You F. Life cycle assessment and technoeconomic analysis of thermochemical conversion technologies applied to poultry litter with energy and nutrient recovery. *ACS Sustainable Chemistry & Engineering*, 2020, 8(22): 8436-8447.
- [4] Mariyam S, Shahbaz M, Al-Ansari T, Mackey H R, McKay G. A critical review on co-gasification and co-pyrolysis for gas production. *Renewable and Sustainable Energy Reviews*, 2022, 161: 112349-68.
- [5] Zhang W, Chen J, Fang H, Zhang G, Zhu Z, Xu W, et al. Simulation on co-gasification of bituminous coal and industrial sludge in a downdraft fixed bed gasifier coupling with sensible heat recovery, and potential application in sludge-to-energy. *Energy*, 2022, 243: 123052-65.
- [6] Zhang W, Huang S, Wu S, Wu Y, Cao J. Ash fusion characteristics and gasification activity during biomasses co-gasification process. *Renewable Energy*, 2020, 147: 1584-1594.
- [7] Mazaheri N, Akbarzadeh A H, Madadian E, Lefsrud M. Systematic review of research guidelines for numerical simulation of biomass gasification for bioenergy production. *Energy conversion and management*, 2019, 183: 671-688.
- [8] Sharma P, Gupta B, Pandey M, Bisen K S, Baredar P. Downdraft biomass gasification: A review on concepts, designs analysis, modelling and recent advances. *Materials Today: Proceedings*, 2021, 46: 5333-5341.
- [9] Bhoi P R, Huhnke R L, Kumar A, Indrawan N, Thapa S. Co-gasification of municipal solid waste and biomass in a commercial scale downdraft gasifier. *Energy*, 2018, 163: 513-518.
- [10] Anniwaer A, Chaihad N, Zhang M, Wang C, Yu T, Kasai Y, et al. Hydrogen-rich gas production from steam co-gasification of banana peel with agricultural residues and woody biomass. *Waste Management*, 2021, 125: 204-214.
- [11] Masmoudi M A, Halouani K, Sahraoui M. Comprehensive experimental investigation and numerical modeling of the combined partial oxidation-gasification zone in a pilot downdraft air-blown gasifier. *Energy Conversion and Management*, 2017, 144: 34-52.
- [12] Lu D, Yoshikawa K, Ismail T M, El-Salam M A. Assessment of the carbonized woody briquette gasification in an updraft fixed bed gasifier using the Euler-Euler model. *Applied energy*, 2018, 220: 70-86.
- [13] Lewin C S, de Aguiar Martins A R F, Pradelle F. Modelling, simulation and optimization of a solid residues downdraft gasifier: application to the co-gasification of municipal solid waste and sugarcane bagasse. *Energy*, 2020, 210: 118498.
- [14] Khodaei H, Al-Abdeli Y M, Guzzomi F, Yeoh G H. An overview of processes and considerations in the modelling of fixed-bed biomass combustion. *Energy*, 2015, 88: 946-972.
- [15] Ngamsidhipongsa N, Ponpesh P, Shotipruk A, Arpornwichanop A. Analysis of the Imbert downdraft gasifier using a species-transport CFD model including tar-cracking reactions. *Energy Conversion and Management*, 2020, 213: 112808.
- [16] Yao Z, You S, Ge T, Wang C. Biomass gasification for syngas and biochar co-production: Energy application and economic evaluation. *Applied Energy*, 2018, 209: 43-55.
- [17] Gómez M A, Porteiro J, Patiño D, Míguez J L. Fast-solving thermally thick model of biomass particles embedded in a CFD code for the simulation of fixed-bed burners[J]. *Energy Conversion and Management*, 2015, 105: 30-44.